Universität Rostock Traditio et Innovatio

COMSOL CONFERENCE 2016 MUNICH

Model Order Reduction using the COMSOL Multiphysics® Software - A Compact Model of a Wireless Power Transfer System

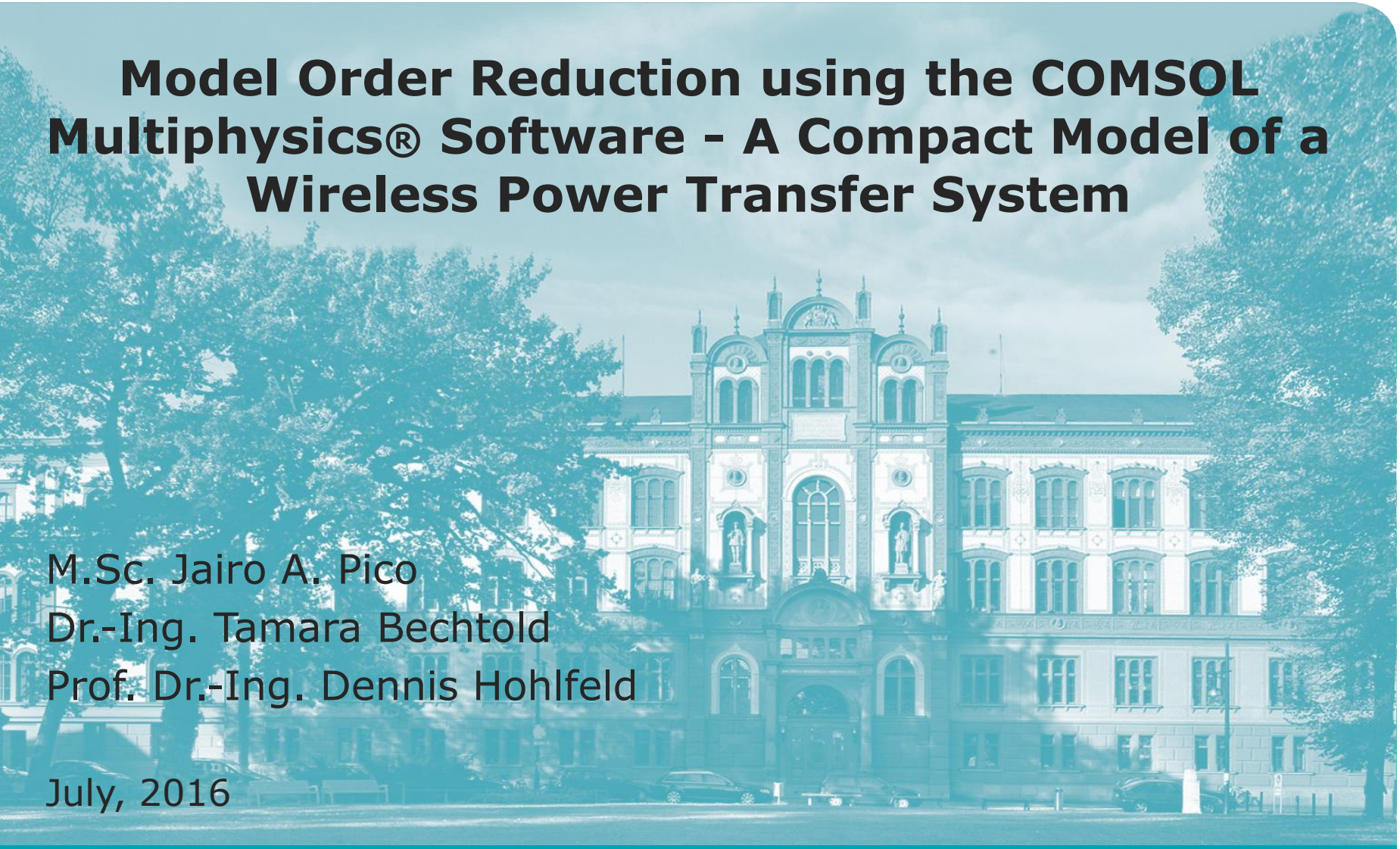

M.Sc. Jairo A. Pico
Dr.-Ing. Tamara Bechtold
Prof. Dr.-Ing. Dennis Hohlfeld

July, 2016

Outline

- Introduction
- Fundamentals
- Model Order Reduction
- Numerical Modelling
- Results
- Conclusions and Outlook

Resonant Inductive Coupling

- Improved power transfer efficiency by using resonant circuits(i.e. a series/parallel capacitor for each coil)
- Greater distances in the range of meters can be covered.

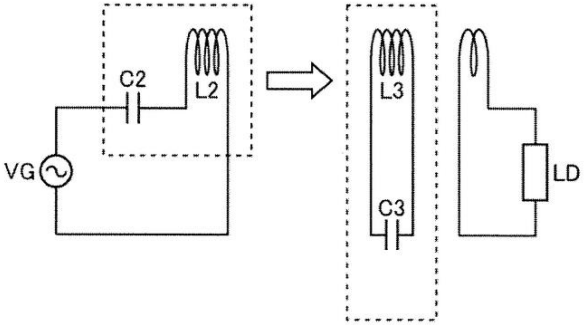

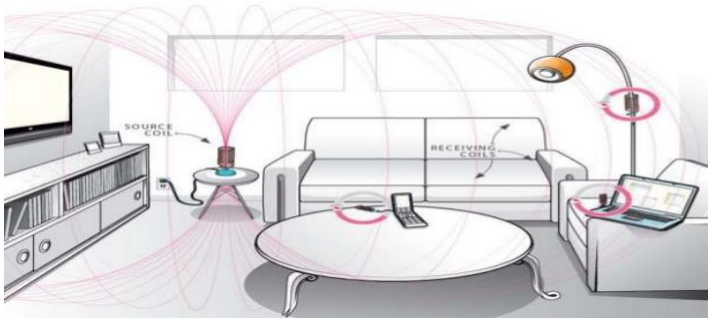

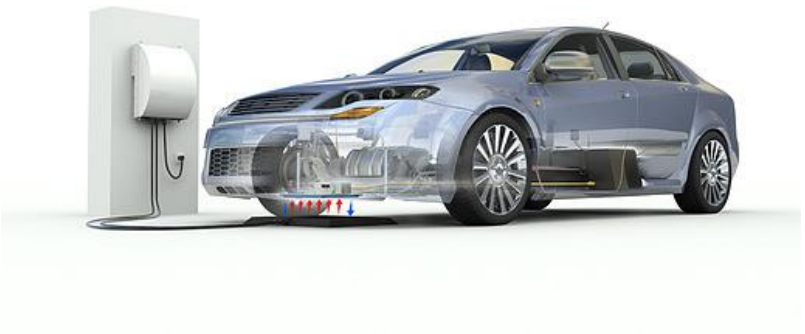

- Interference in radio communications can be introduced.
- Further studies are needed in regard of human exposure to electromagnetic fields.

Introduction

The company IPT-Technology wirelessly charging buses equipped with receiver coils, which are energized as they stop or park over powered pads, those embedded in the roadway or in the garage floor.

Since 2002, its buses are serving along the cities of Turin and Genoa.

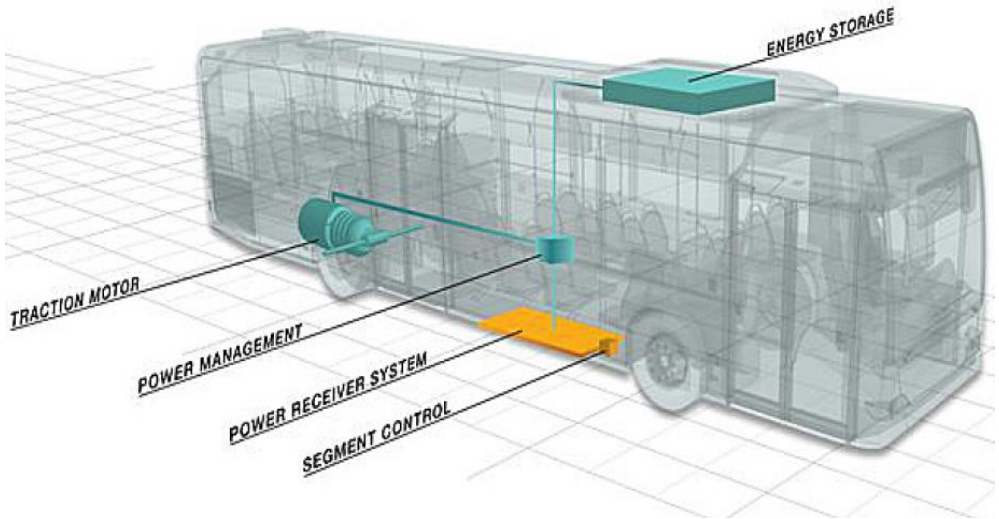

The company Bombardier also developed a suite of e-mobility solutions for electric transit, containing on-board light batteries.

Currently some deployments of their WPT buses are underway in Mannheim and Berlin, Germany, as well as in Bruges, Belgium.

Introduction

In 2009, Bombardier introduced an WPT Rail Tram in Augsburg, Germany.

The system deliver a power output in the range of 100-500 kW at 200 kHz, the tram achieves up to 90 km/h..

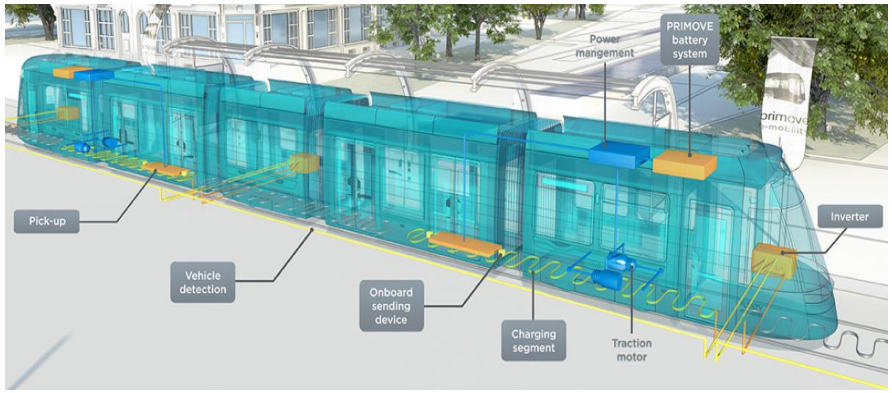

Companies HELLA and VAHLE work together with two approaches in cars:

- locating the coils beneath the car,
- a coil surrounding the frontal license plate, while the other in a pole.

Several configurations for the coils are developed: bipolar solenoid, unipolar rectangular and bipolar rectangular, for systems delivering up to 3.7 kW.

Distance between coils in the range of 80-250 mm, and with an axis misalignment lower than 100 mm.

Introduction

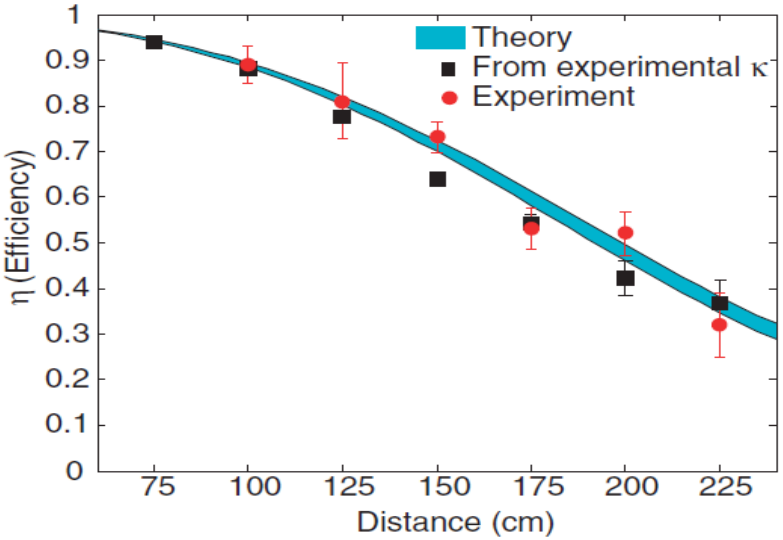

In 2007, an initial report demonstrated efficient WPT over distances up to eight times the radius of the coil.

Approximately 40% of efficiency was reached over distances in excess of two meters.

In 2010, a work with helical coils was presented, allegedly providing a better approach between the analytical model and its experimental counterpart.

It was informed that power efficiency was up to 87% at a distance of 75 cm, with a resonant frequency of 10 MHz.

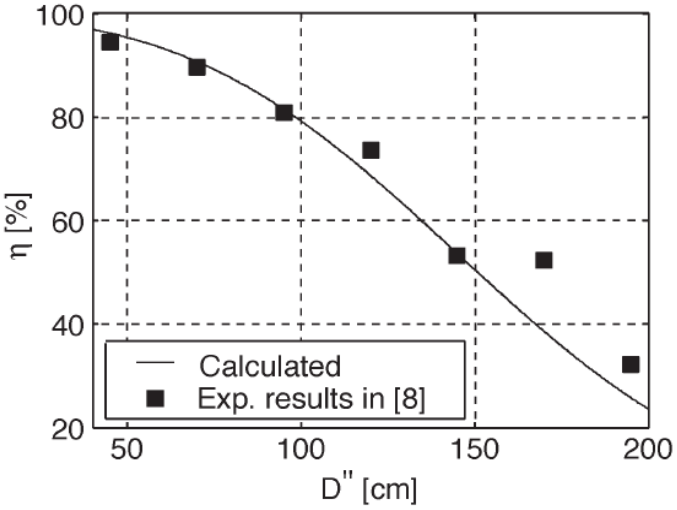

Introduction

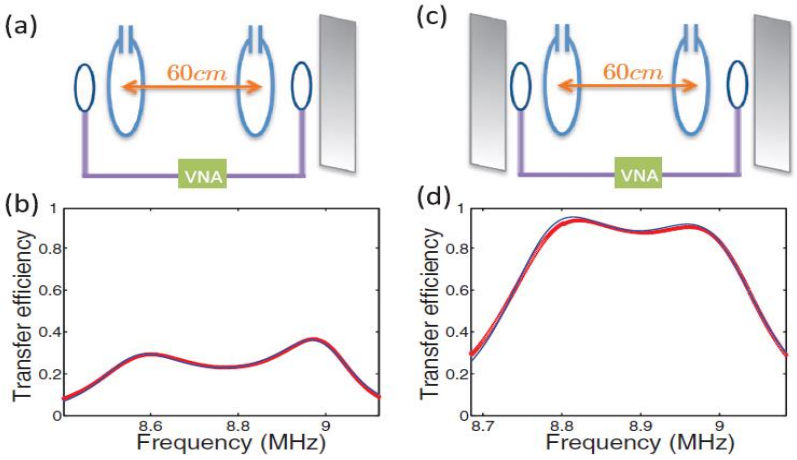

In 2013, an experiment is conducted in regard of measuring the efficiency when aluminium plates are placed behind the resonators.

Efficiency greater than 96% was delivered in a distance of 60 cm, for a resonator with a coil radius of 30 cm at 8.4 MHz.

In 2014, a full recharging system is reported for EVs, the circuit is operated at 400 VDC and a frequency range between 10 to 200 kHz.

The system consisted of a couple of rectangle coils each attached to a ferrite layer, avoiding that any magnetic field flux reaches the car, which were also covered by an shield aluminum plate.

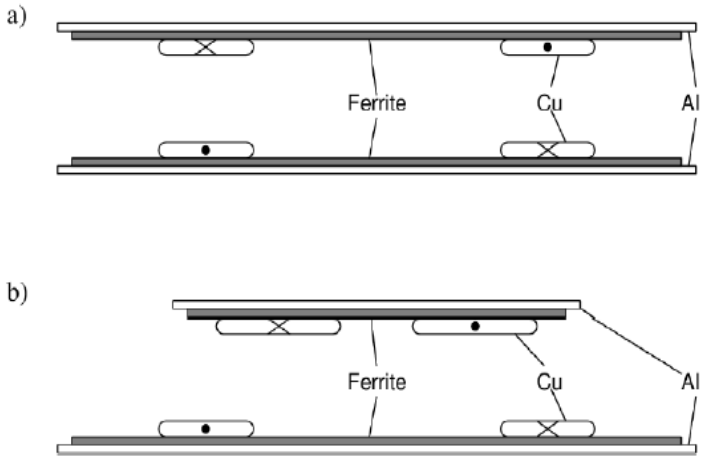

Outline

- Introduction
- Fundamentals
- Model Order Reduction
- Numerical Modelling
- Results
- Conclusions and Outlook

WPT circuit analysis

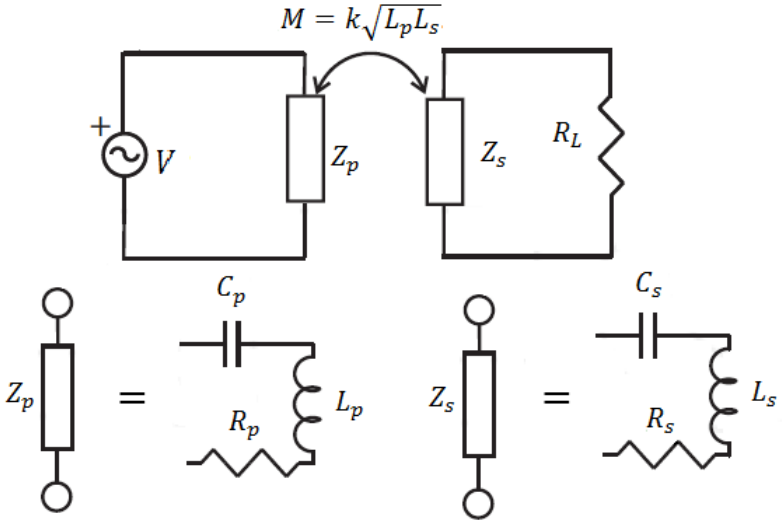

When a pair of coils are apart from each other, their resonance frequencies are:

$$\omega_p = \frac{1}{\sqrt{L_p C_p}} \text{ , } \omega_s = \frac{1}{\sqrt{L_s C_s}}$$

However, as they are placed near, their coupling coefficient $k > 0$, Both coils are coupled magnetically, through the mutual inductance $M = k\sqrt{L_p L_s}$, and can exchange energy, as the lumped circuit represented in the diagram.

WPT circuit analysis (Cont'd)

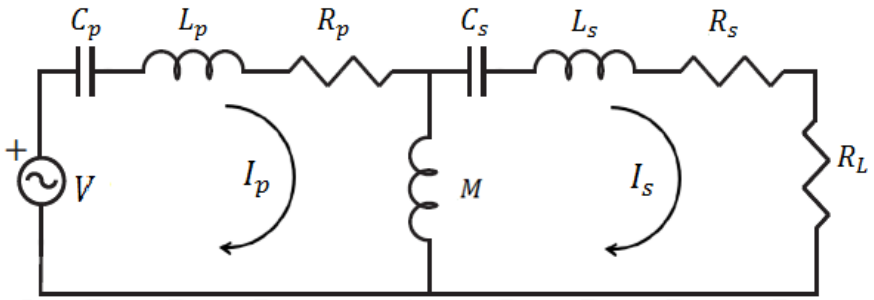

An equivalent lumped circuit can be elaborated, since the mutual inductance *M* can be represented as a coupled inductance, between primary and secondary resonators.

The Kirchhoff's Voltage Law (KVL) equations for primary and secondary circuits can be formulated straightforward from the circuit .

$$\begin{bmatrix} Z_p & j\omega M \\ j\omega M & Z_s + R_L \end{bmatrix} \begin{bmatrix} I_p \\ I_s \end{bmatrix} = \begin{bmatrix} V \\ 0 \end{bmatrix}$$

$$I_p = \frac{V(Z_s + R_L)}{Z_p(Z_s + R_L) + (\omega M)^2}$$

$$Z_p = R_p + j\omega L_p + 1/j\omega C_p$$

$$Z_s = R_s + j\omega L_s + 1/j\omega C_s$$

$$I_s = \frac{I_p(-j\omega M)}{(Z_s + R_L)} = \frac{V(-j\omega M)}{Z_p(Z_s + R_L) + (\omega M)^2}$$

Fundamentals

Frequency splitting

$$Z_{in} = \frac{V}{I_p} = \frac{Z_p(Z_s + R_L) + (\omega M)^2}{(Z_s + R_L)}$$

At resonance, reactance of the circuit is zero for input impedance, and thus it yields a fourth degree polynomial with the following solutions, if it is assumed that $R_L = R_p = R_s = 0$:

$$\omega_{1,2,3,4} = \pm \sqrt{\frac{\omega_p^2 + \omega_s^2 \pm \sqrt{\left(\omega_p^2 + \omega_s^2\right)^2 - 4\omega_p^2\omega_s^2(1-k^2)}}{2(1-k^2)}}$$

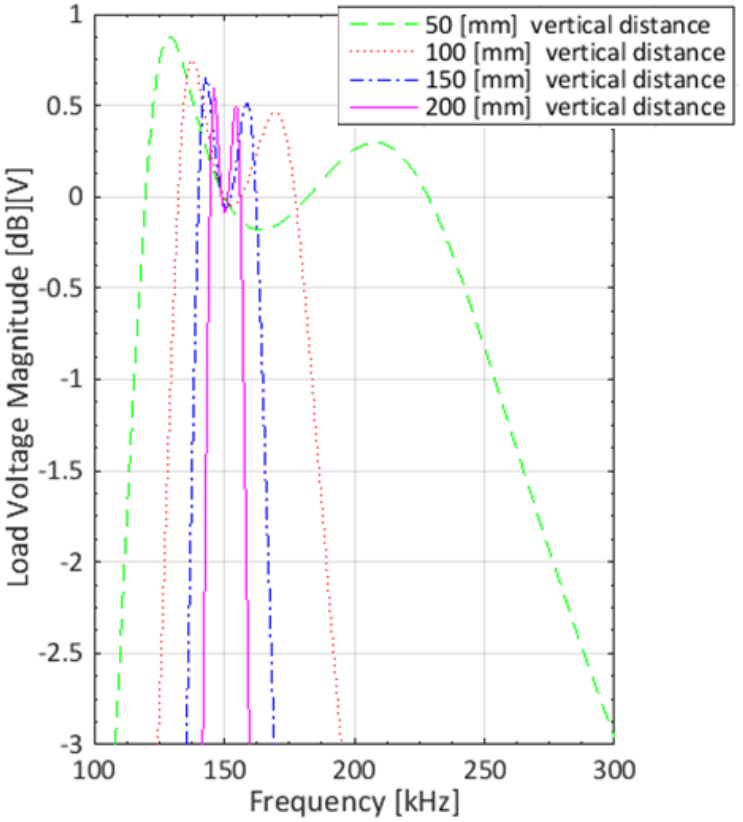

In case both resonant frequencies are set to the same value $\omega_p = \omega_s = \omega_0$, then only two solutions are yielded:

$$\omega_{1,2} = \frac{\omega_0}{\sqrt{1 \pm k}}$$

Fundamentals

Power transfer efficiency

Defined as the ratio of the output power P_{out} divided by the input power P_{in}:

$$\eta = \frac{P_{out}}{P_{in}} = \frac{(\omega M)^2 R_L}{(Z_s + R_L)\left(Z_p(Z_s + R_L) + (\omega M)^2\right)}$$

$$U = \frac{\omega M}{\sqrt{R_p R_s}} = \omega k \sqrt{\frac{L_p L_s}{R_p R_s}}$$

$$\eta = \frac{U^2}{\left(\frac{R_s}{R_L} + 1\right)\left[\left(1 + \frac{R_L}{R_s}\right) + U^2\right]}$$

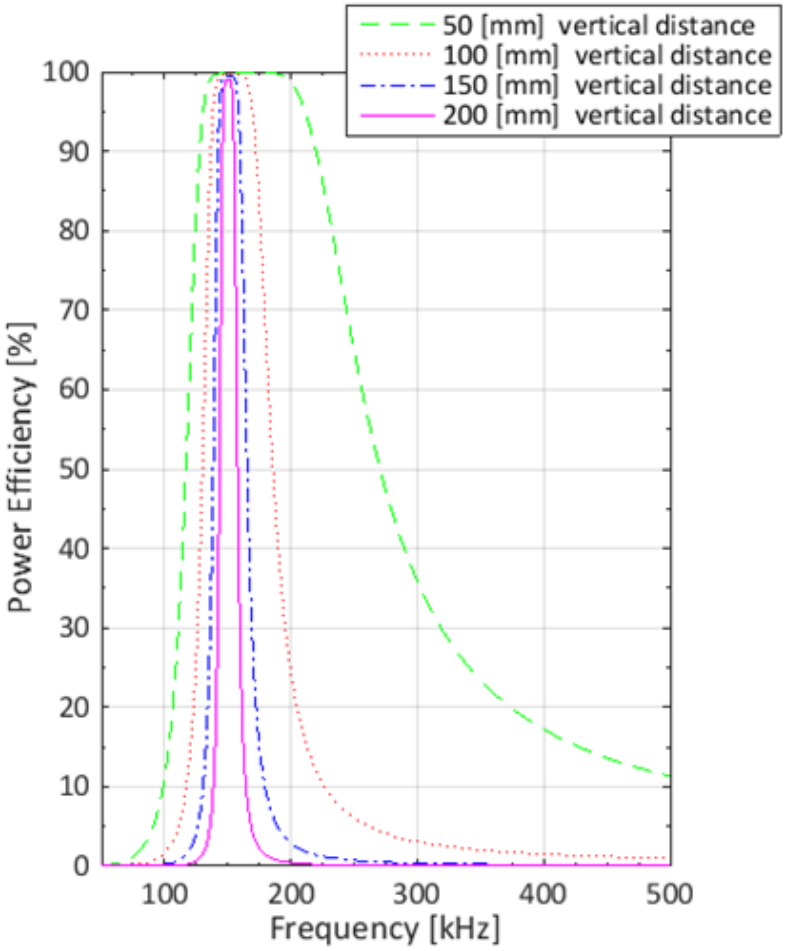

Numerical modeling by using Finite Element Method (FEM)

Ampère's law is used for solving problems in electrical and magnetism fields, which can be expressed in terms of the magnetic vector potential $\vec{A}$:

$$\nabla \times \vec{H} = \nabla \times \left(\frac{\vec{B}}{\mu_0}\right) = \nabla \times \left(\frac{1}{\mu_0}\nabla \times \vec{A}\right) = j\omega\vec{D} + \vec{J}$$

$$\vec{J} = \sigma\vec{E} + \vec{J}_e$$

$$\vec{D} = -\varepsilon_0\vec{E} \quad \Rightarrow \quad \nabla \times \left(\frac{1}{\mu_0}\nabla \times \vec{A}\right) = (j\omega\varepsilon_0 + \sigma)\vec{E} + \vec{J}_e = (\omega^2\varepsilon_0 - j\omega\sigma)\vec{A} - (j\omega\varepsilon_0 + \sigma)\nabla V + \vec{J}_e$$

$$\vec{E} = -\nabla V - j\omega\vec{A}$$

$$(j\omega\sigma - \omega^2\varepsilon_0)\vec{A} + \nabla \times \left(\frac{1}{\mu_0}\nabla \times \vec{A}\right) + (j\omega\varepsilon_0 + \sigma)\nabla V = \vec{J}_e$$

$\vec{H}$: magnetic field strength
$\vec{B}$:magnetic field
$\vec{D}$:electric displacement field
$\vec{E}$: electric field
$\vec{J}$: total current density
V: electric potential.
$\vec{J}_e$: source current density
μ_0:permeability constant
σ: conductivity
ε_0: permittivity constant
I_{coil}: current flowing in the coil

Multi-turn Coil: $J_e = \frac{NI_{coil}}{A}$

Outline

- Introduction
- Fundamentals
- Model Order Reduction
- Numerical Modelling
- Results
- Conclusions and Outlook

Model Order Reduction

First order systems

$$E\,\dot{x}(t) = A\,x(t) + B\,u(t)$$

$$y(t) = C\,x(t) + D\,u(t)$$

E: $n \times n$, A: $n \times n$, B: $n \times m$, C: $p \times n$, D: $p \times m$

$$E_r\,\dot{x}_r(t) = A_r\,x_r(t) + B_r\,u(t)$$

$$y(t) = C_r\,x_r(t) + D\,u(t)$$

E_r: $k \times k$, A_r: $k \times k$, B_r: $k \times m$, C_r: $p \times k$, D: $p \times m$

Model Order Reduction

Transfer function of first order systems

$$\frac{Y(s)}{U(s)} = H(s) = C(A^{-1}Es - I)^{-1}A^{-1}B + D$$

By using Neumann Expansion:

$$(A^{-1}Es - I)^{-1} = -I - (A^{-1}E)s - (A^{-1}E)^2s^2 + \cdots = -\sum_{i=0}^{\infty}(A^{-1}E)^i s^i$$

$$H(s) = -CA^{-1}B - C(A^{-1}E)A^{-1}Bs - C(A^{-1}E)^2A^{-1}Bs^2 - \cdots$$

Moments of H(s):

$$M_i = C(A^{-1}E)^i A^{-1}B\,, \qquad i = 0,1\ldots$$

Model Order Reduction

Approximation by Projection.

Orthogonal projection of a vector onto another vector

$$\vec{e} = \vec{b} - \vec{p}$$
$$\vec{e} \perp \vec{a}\,, \vec{a}^T\vec{e} = \vec{0}$$

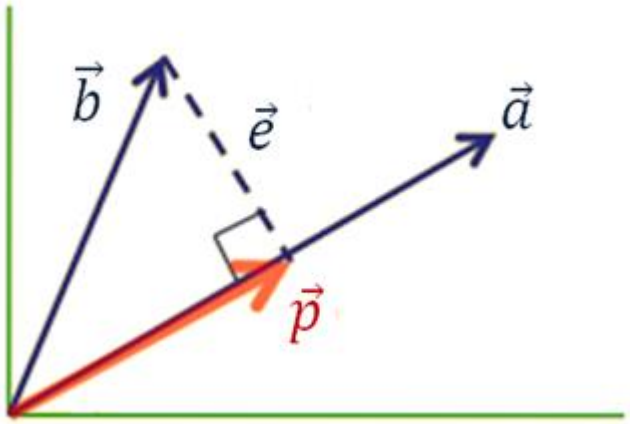

$$P\vec{b} = \vec{p} = \xi\vec{a}$$

$$\vec{a}^T\vec{e} = \vec{a}^T\left(\vec{b} - \hat{p}\right) = \vec{a}^T\left(\vec{b} - \xi\vec{a}\right) = \vec{a}^T\vec{b} - \xi\vec{a}^T\vec{a} = \hat{0}$$

$$\xi = \frac{\vec{a}^T\vec{b}}{\vec{a}^T\vec{a}}$$

Model Order Reduction

Approximation by Projection.

Orthogonal projection of a vector onto a plane

$$\vec{e} = \vec{b} - \vec{p}$$

$$A^T\vec{e} = \vec{0}$$

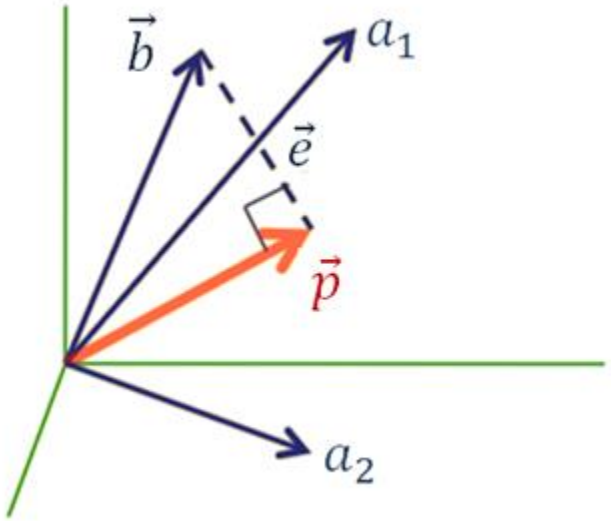

$$A = \begin{bmatrix} \uparrow & \uparrow \\ a_1 & a_2 \\ \downarrow & \downarrow \end{bmatrix}$$

$$P\vec{b} = x_1 \begin{bmatrix} \uparrow \\ a_1 \\ \downarrow \end{bmatrix} + x_2 \begin{bmatrix} \uparrow \\ a_2 \\ \downarrow \end{bmatrix} = A\vec{x} = \vec{p}$$

$$A^T\vec{e} = A^T\left(\vec{b} - \vec{p}\right) = A^T\left(\vec{b} - A\vec{x}\right) = 0$$

$$A^T\vec{b} = A^TA\vec{x}$$

$$\vec{x} = (A^TA)^{-1}A^T\vec{b}$$

$$P\vec{b} = A\vec{x} = A(A^TA)^{-1}A^T\vec{b}$$

$$P = A(A^TA)^{-1}A^T$$

Model Order Reduction

Approximation by Projection.

General Projection of a Vector

$$\vec{x}_\perp = \vec{x} - \vec{x}_p$$

$$W^T \vec{x}_\perp = 0$$

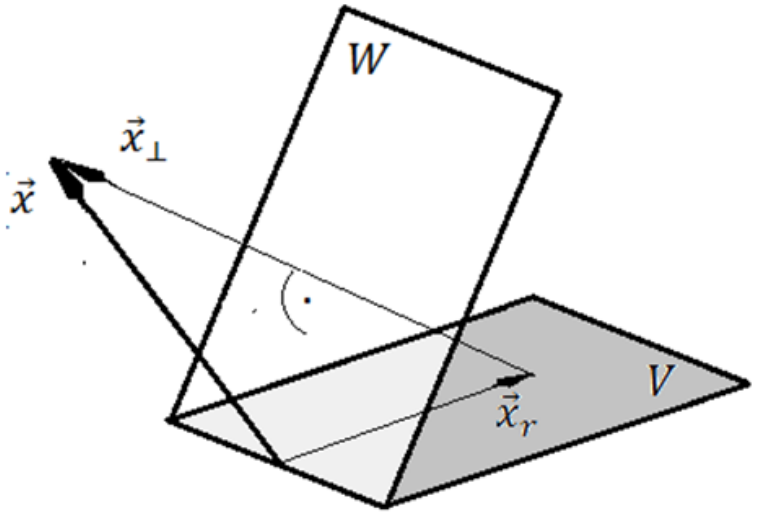

$$V = \begin{bmatrix} \uparrow & & \uparrow \\ v_1 & \dots & v_k \\ \downarrow & & \downarrow \end{bmatrix}$$

$$P\vec{x} = V\vec{x}_r = \vec{x}_p$$

$$W^T \vec{x}_\perp = W^T\left(\vec{x} - \vec{x}_p\right) = W^T(\vec{x} - V\vec{x}_r) = 0$$

$$W^T \vec{x} = W^T V \vec{x}_r$$

$$\vec{x}_r = (W^T V)^{-1} W^T \vec{x}$$

$$P\vec{x} = V\vec{x}_r = V(W^T V)^{-1} W^T \vec{x}$$

$$P = V(W^T V)^{-1} W^T$$

Model Order Reduction

Approximation by Projection.

$$\underset{n\times n}{A}\, x(t) = \underset{n\times n}{A}\,\underset{n\times k}{V}\, x_r(t) + \varepsilon$$

$$\underset{k\times n}{W^T}\,\underset{n\times n}{A}\, x(t) = \underset{k\times n}{W^T}\,\underset{n\times n}{A}\,\underset{n\times k}{V}\, x_r(t) + \underset{k\times n}{W^T}\,\varepsilon$$

$$E_r = W^T E V$$
$$A_r = W^T A V$$
$$B_r = W^T B$$
$$C_r = C V$$

Model Order Reduction

Approximation by Projection. (Cont'd)

$$W^T_{k\times n}\; E_{n\times n}\; V_{n\times k}\;\dot{x}_r(t) = W^T_{k\times n}\; A_{n\times n}\; V_{n\times k}\; x_r(t) + W^T_{k\times n}\; B_{n\times m}\; u(t)$$

$$y(t) = C_{p\times n}\; V_{n\times k}\; x_r(t) + D_{p\times m}\; u(t)$$

$$E_r = W^T E V$$
$$A_r = W^T A V$$
$$B_r = W^T B$$
$$C_r = C V$$

$$E_r{}_{k\times k}\;\dot{x}_r(t) = A_r{}_{k\times k}\; x_r(t) + B_r{}_{k\times m}\; u(t)$$

$$y(t) = C_r{}_{p\times k}\; x_r(t) + D_{p\times m}\; u(t)$$

Model Order Reduction

Second Order Systems

$$\begin{cases} M\ddot{x}(t) + E\dot{x}(t) + Kx(t) = Fu(t) \\ y = C_v\dot{x}(t) + C_p x(t) + Du(t) \end{cases}$$

$$M, E, K \in \mathbb{R}^{n\times n}, F \in \mathbb{R}^{n\times m}, C_v, C_p \in \mathbb{R}^{p\times n}, D \in \mathbb{R}^{p\times m}, u \in \mathbb{R}^m, x \in \mathbb{R}^n, y \in \mathbb{R}^p$$

$$E\dot{x}(t) = Ax(t) + Bu(t)$$
$$y(t) = Cx(t) + Du(t)$$

$$\begin{cases} \begin{bmatrix} P & 0 \\ 0 & M \end{bmatrix} \begin{pmatrix} \dot{z}(t) \\ \ddot{z}(t) \end{pmatrix} = \begin{bmatrix} 0 & P \\ -K & E \end{bmatrix} \begin{bmatrix} z(t) \\ \dot{z}(t) \end{bmatrix} + \begin{bmatrix} 0 \\ F \end{bmatrix} u(t) \\ y(t) = [C_p \quad C_v] \begin{bmatrix} z(t) \\ \dot{z}(t) \end{bmatrix} + Du(t) \end{cases}$$

$$E = \begin{bmatrix} P & 0 \\ 0 & M \end{bmatrix}, x(t) = \begin{bmatrix} z(t) \\ \dot{z}(t) \end{bmatrix}, A = \begin{bmatrix} 0 & P \\ -K & E \end{bmatrix}, B = \begin{bmatrix} 0 \\ F \end{bmatrix}, C = [C_p \quad C_v]$$

$P \in \mathbb{R}^{n\times n}$ is a non-singular matrix, and its choice is optional and has no effect on the results

Model Order Reduction

Arnoldi Method (Cont'd)

Algorithm 1 **. Arnoldi Iteration**

Input: Matrix P, starting vector $\vec{q}$

Output: Matrix H, V

1: $\vec{v}_1 = \vec{q}/\|\vec{q}\|_2$

2: ***for*** $n = 1, 2, \ldots$ ***do***

3: $\quad \vec{r} = P\vec{v}_n$

4: $\quad$ ***for*** $j = 1, \ldots, n$ ***do***

5: $\quad\quad h_{j,n} = \vec{v}_j{}^T \cdot \vec{r}$

6: $\quad\quad \vec{r} = \vec{r} - h_{j,n}\vec{v}_j$

7: $\quad$ ***end for***

8: $\quad h_{n+1,n} = \|r\|_2$

9: $\quad \vec{v}_{n+1} = r/h_{n+1,n}$

$$\mathcal{K}_n = \langle \vec{q}, P\vec{q}, \ldots, P^{n-1}\vec{q} \rangle = \langle \vec{v}_1, \vec{v}_2, \ldots, \vec{v}_n \rangle \subseteq \mathbb{C}^m$$

$$\mathcal{K}_n = \left[\vec{q} \,\middle|\, P\vec{q} \,\middle|\, \ldots \,\middle|\, P^{n-1}\vec{q} \right]$$

$$\mathcal{K}_k\left(A^{-1}E,\ A^{-1}\vec{b} \right) = span\left\{ A^{-1}\vec{b}, (A^{-1}E)A^{-1}\vec{b}, \ldots, (A^{-1}E)^{n-1}A^{-1}\vec{b} \right\}$$

$$P = A^{-1}E,\ \vec{q} = A^{-1}\vec{b}$$

$$\mathcal{K}_k\left(A^{-T}E^T,\ A^{-T}\vec{c} \right) = span\left\{ A^{-T}\vec{c},\ (A^{-T}E^T)A^{-T}\vec{c}, \ldots,\ (A^{-T}E^T)^{k-1}A^{-T}\vec{c} \right\}$$

$$P = A^{-T}E^T,\ \vec{q} = A^{-1}\vec{c}$$

Outline

- Introduction
- Fundamentals
- Model Order Reduction
- Numerical Modelling
- Results
- Conclusions and Outlook

Numerical Modelling

2D Models: Pair of Disc Coils & Windings with Concentric Coils

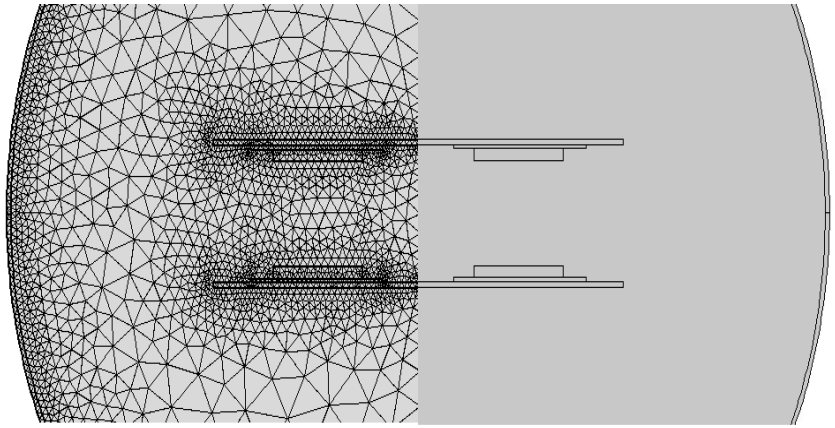

Selection of Multi-Turn-Coil Feature for a simple geometry, offers a handy and practical approach, as this geometry will be considered a bundle of tiny wire tightly bounded together but isolated by an electrical insulator, and the current will flow only in the direction of the wires

Inner rectangles correspond to each winding coil, with its corresponding ferrite core and aluminium shield plate.

The air is represented in the model by the surrounding circle. Since is a 2D Axis-symmetric model, only the right half portion of the system needs to be created.

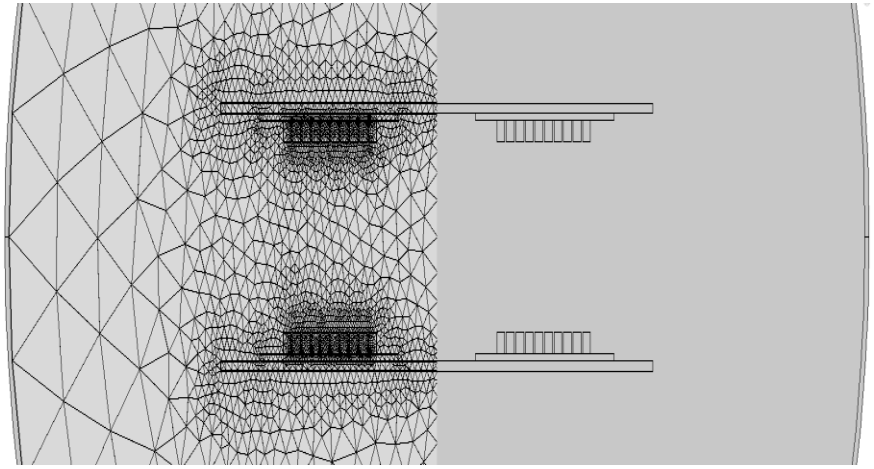

Numerical Modelling

3D model: Pair of Disc Coils

Despite a 3D model offers a more realistic approach to the system, and more accurate results, its DoF is dramatically increased, and thus the calculation time is also extended.

The complexity of the model might also affect the convergence to a solution.

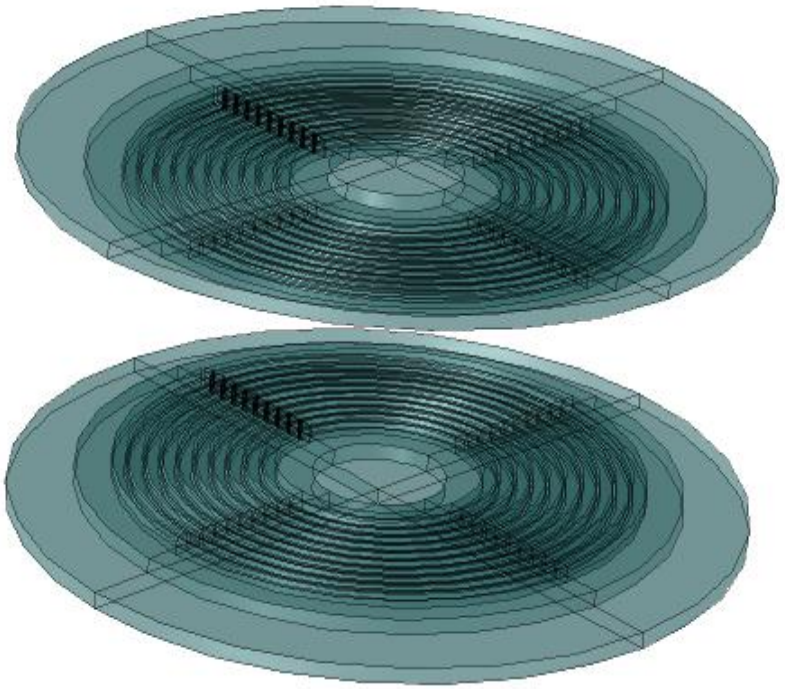

Nevertheless, some features are only reproduced in 3D scenario, since they are simply not possible for an 2D axis-symmetric system.

For instance, a vertical displacement between coils is possible to be modelled in the 2D model, however it is not the case for a horizontal displacement

Outline

- Introduction
- Fundamentals
- Model Order Reduction
- Numerical Modelling
- Results
- Conclusions and Outlook

Results

Sensitivity analysis of reduced models

The following analysis was focused in comparing the accuracy of the block Arnoldi algorithms that were implemented against the results generated by running the original model in Comsol.

Parameter	Value
Name Model	3D Disc Coils
Degrees of freedom	131.829
Range of frequency	10-500 kHz
Vertical displacement	100 mm
Horizontal displacement	0 mm
Output variables	Resistance in first coil and mutual inductance
Block Arnoldi algorithms	Input-Sided, Output-Sided and Two-Sided SOAR
MOR expansion point	1 kHz
Number of Moments	4, 5 , 6 and 7 moments

Results

Sensitivity analysis of reduced models

- Run original model in Comsol and save data in CSV file format.
- Extract the state-space matrices of the model from Comsol by using Matlab.
- Perform MOR of the matrices by using every of the block Arnoldi algorithms
- By using the reduced matrices, calculate the output variables for the range of frequency, and its corresponding relative error against the results that were produced by the original model.

Results

Sensitivity analysis of reduced models

By reducing with block input-sided SOAR

All the reduced models with more than 4 moments were reliable, however only up to 150 kHz, when the error started to increase with a steeper slope for the reduced models with 5 and 6 moments.

Finally, for the case of reduced model with 7 moments, the error is lower than 2.5 % for all the range of frequency.

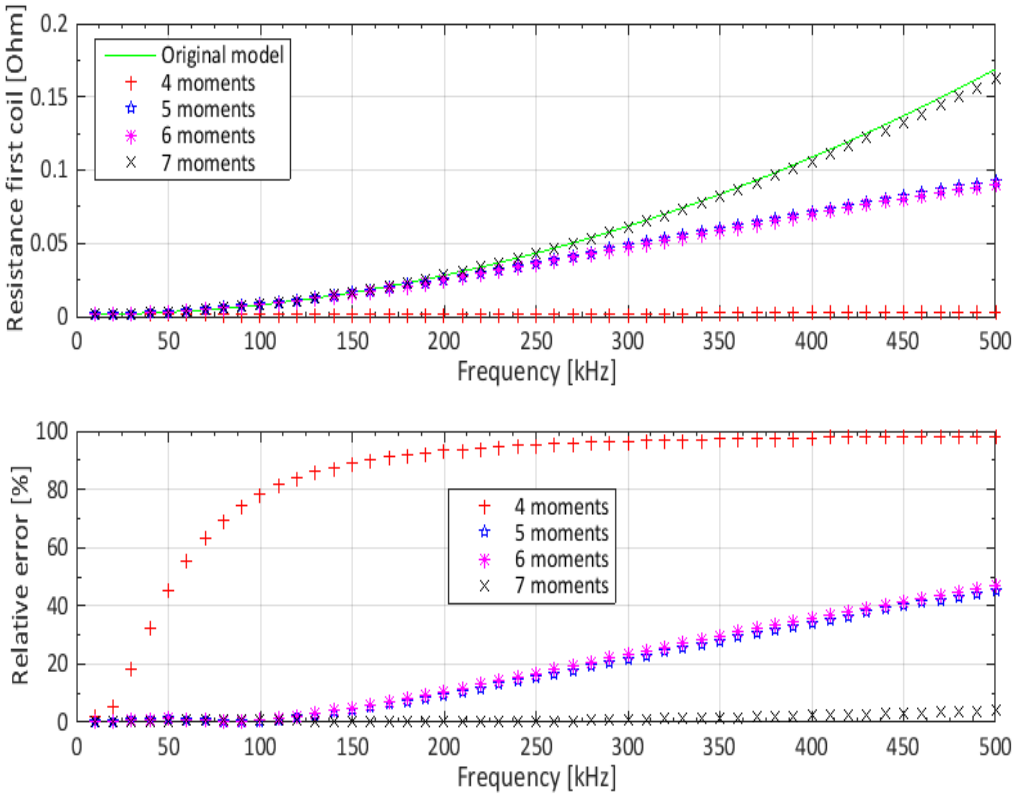

Results

Sensitivity analysis of reduced models

By reducing with block output-sided SOAR

Even the 4-moments model produces better results than its input-sided counterpart; nonetheless its relative error is near 25 % for high frequencies.

With an acceptable response, reduced systems with 5 and 6 moments score a relative error near 7 % as frequencies become greater than 100 kHz.

The 7-moments reduced system only yields a relative error below 1 % for all the range of frequencies

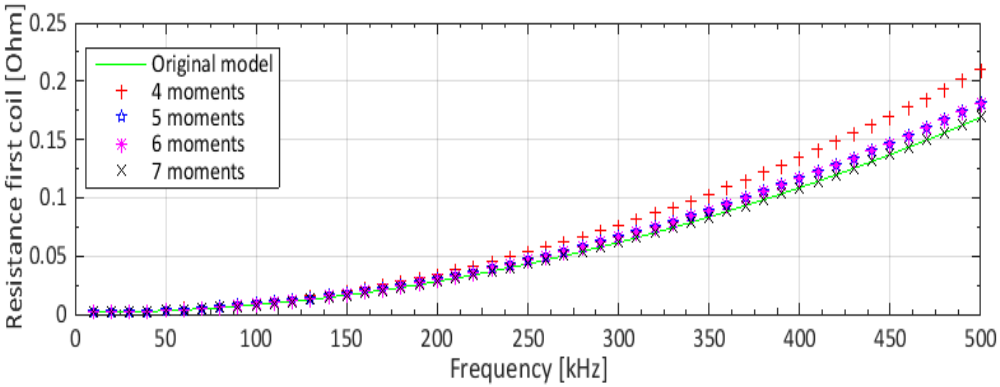

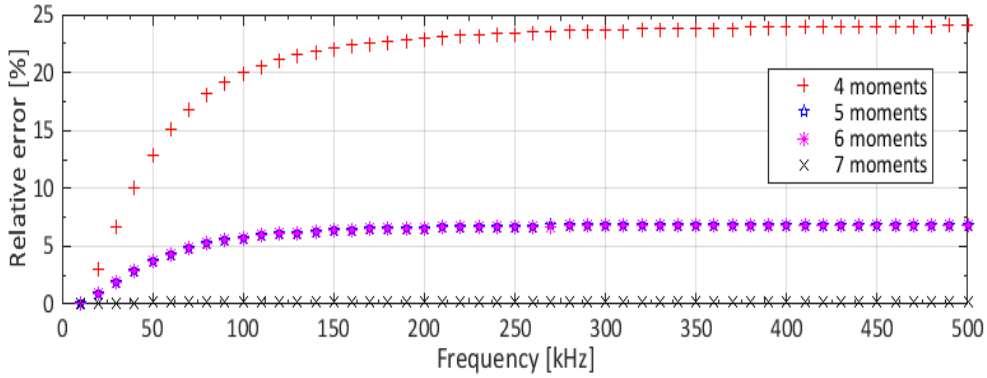

Results

Sensitivity analysis of reduced models

By reducing with block two-sided SOAR

Every reduced model is reliable to the original model's results by using two-sided SOAR, with a maximum error of 5×10^{-3} % for all of them.

Block two-sided SOAR algorithm portrays a great robustness and accuracy, even for models that were created with lower number of moments, not to mention its response is above of those yielded by the one-sided algorithms

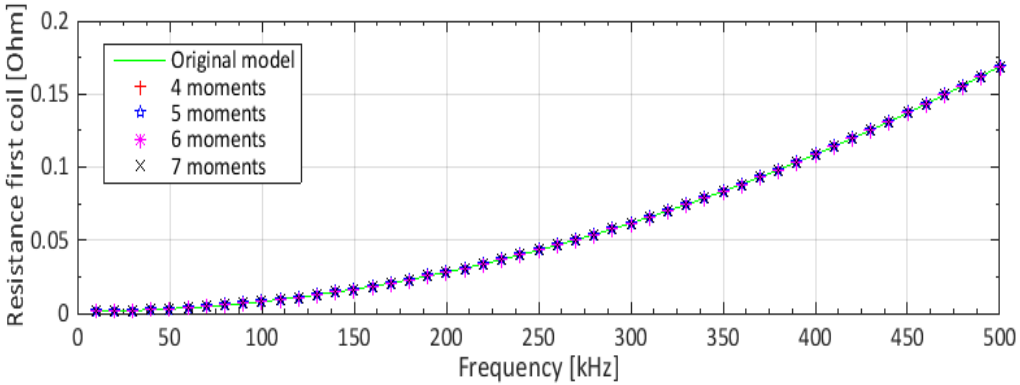

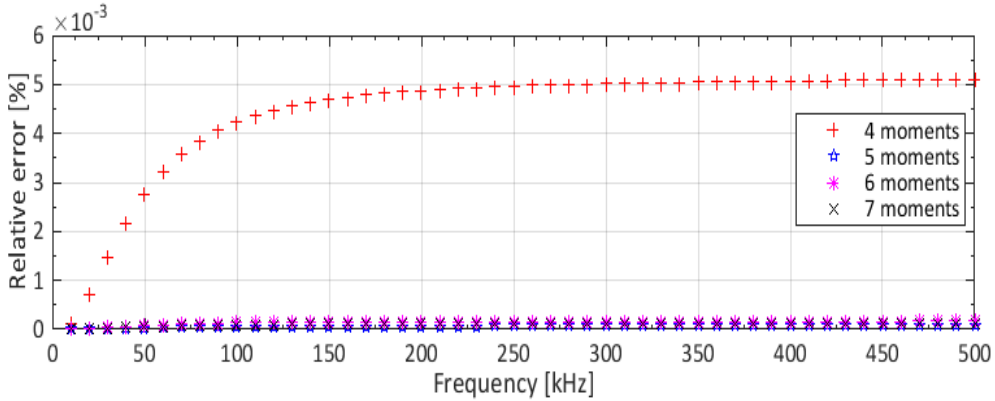

Results

Power efficiency analysis

A power analysis was conducted as a final investigation, which summarizes all the theorical and practical work that was involved on this thesis.

Furthermore, this analysis demanded that the reduced models were exported to Simplorer, and connected to an electric circuit, in such a way that the power efficiency could be measured

Parameter	Value
Name Model	3D Disc Coils
Degrees of freedom	131.829
Desired resonant frequency	150 kHz
Range vertical displacement	25 – 250 mm. Interval increment : 25 mm
Range horizontal displacement	0 - 450 mm. Interval increment: 50 mm
Output variables	Resonant capacitance, optimal load and power efficiency
Block Arnoldi algorithm	Two-Sided SOAR
MOR expansion point	150 kHz
Number of Moments	10 moments
Simplorer's Range of Frequency	0 -500 kHz

Results

Power efficiency analysis

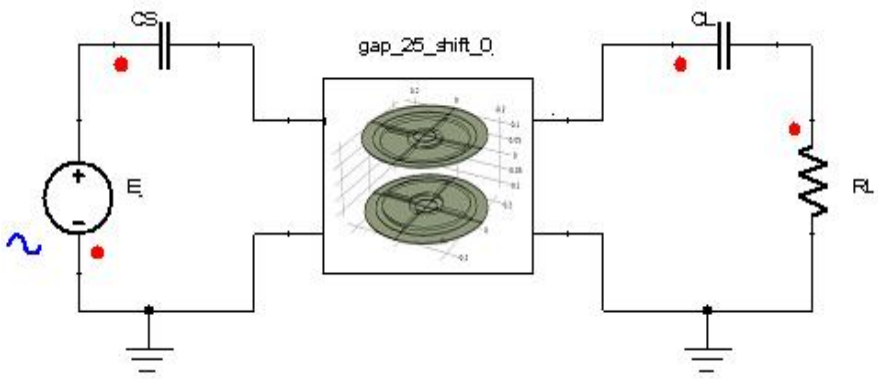

Every set of reduced matrices was saved into a VHDL file, thus, they will represent as a 2-ports electrical circuit. Thereafter, this can be then imported and connected to any extended electric circuits inside Simplorer.

Inductance is calculated for every single set of reduced matrices, and thereafter by using the formula of resonant frequency, the capacitance could be finally determined:

$$\omega = \frac{1}{\sqrt{LC}}$$

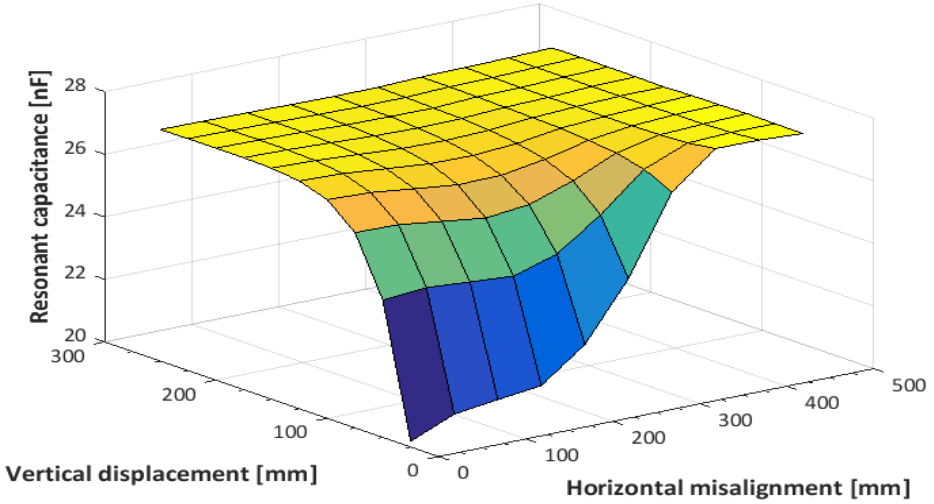

Results

Power efficiency analysis

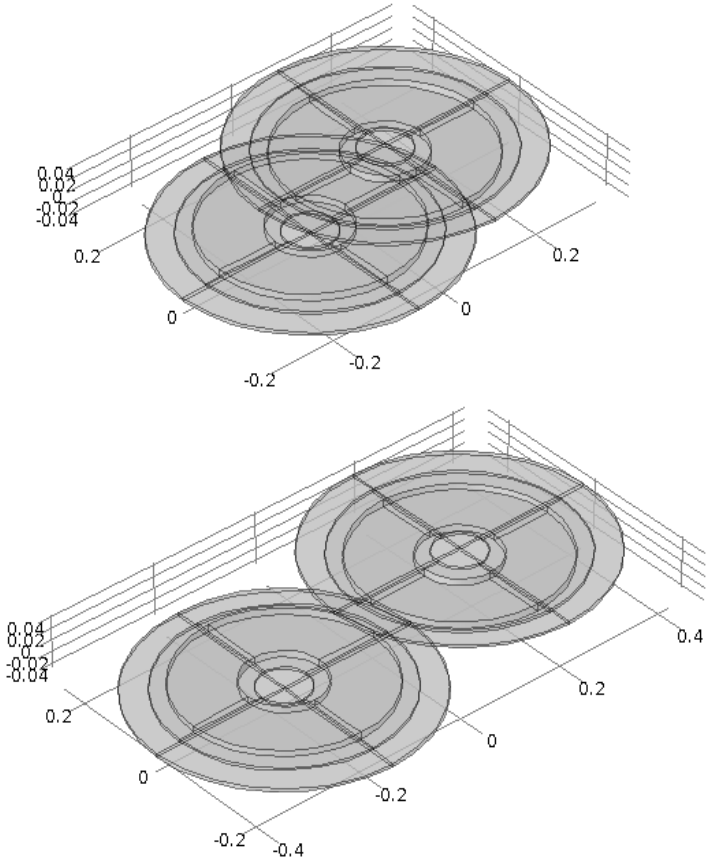

Disc coils with a) 150 mm and b) 350 mm of horizontal misalignment and 50 mm of vertical distance

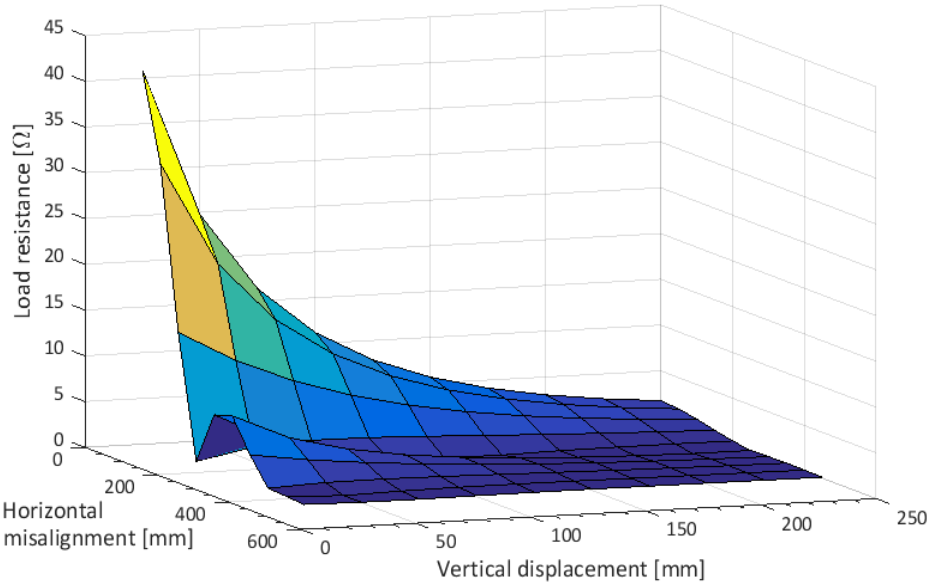

As it is expected, the value of load resistance decreases as vertical or horizontal displacement is increased, however a particular phenomena occurs around the range of 50-250 mm, with a minimum near 150 mm, where the value of optimal load resistance drops near zero.

Results

Power efficiency analysis

A detailed zoom is displayed around the central resonance frequency of 150 kHz and illustrates the WPT frequency splitting.

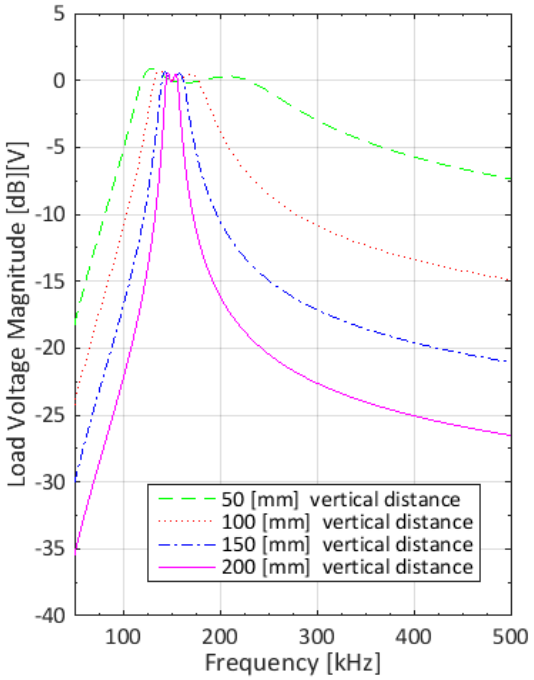

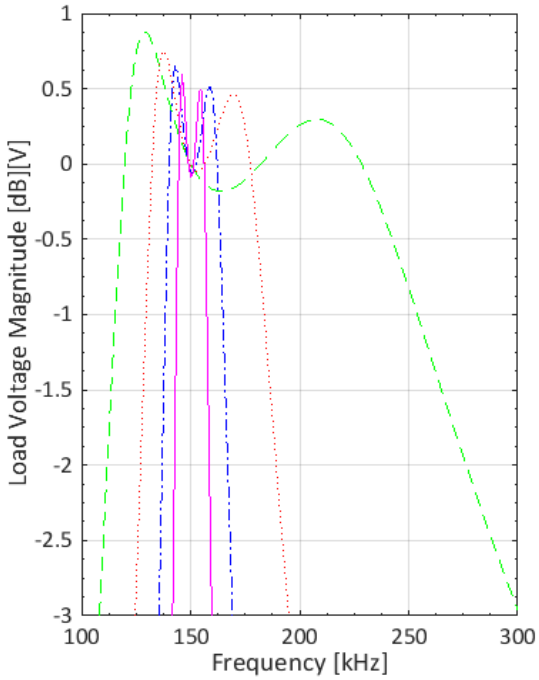

Vertical distance [mm]	$f_0/\sqrt{1+k}$ [kHz]	$f_0/\sqrt{1-k}$ [kHz]
50	119,74	228,53
100	132,34	177,36
150	140,13	162,3
200	144,42	156,28

Table listing the approximated ranges for this frequency splitting, as the circuit resistances are assumed equal to zero

Results

Power efficiency analysis

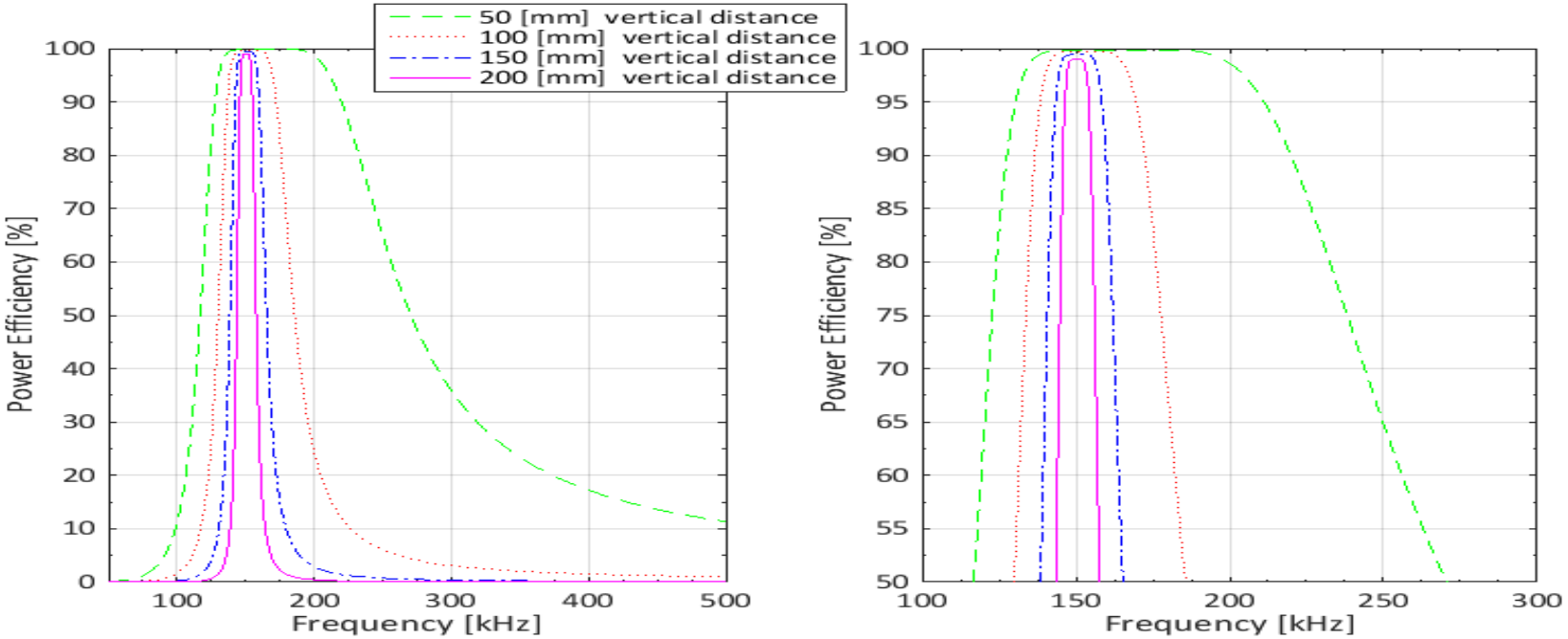

Maximum power efficiency always occurs between the range comprised by the frequency splitting phenomena.

The central resonance frequency always lies in between this range.

The length of the range is affected by the separation between coils.

Outline

- Introduction
- Fundamentals
- Model Order Reduction
- Numerical Modelling
- Results
- Conclusions and Outlook

Conclusions and Outlook

- All elaborated models in Comsol proved their reliability, since they yielded results with an relative error lower than 4 % than those provided by the reference model.
- Even though, 2D models could not be used in analysis with horizontal displacements, they were useful for testing and validating every required step in the conducted experiments.
- For SOAR methods, experiments showed an overall better response and stability of the block two-sided algorithm as being compared with the one-sided methods. Nonetheless, they also showed the overall robustness of all of them, and how with only a handful number of moments, they can reproduce the same response than a full model with more than 10k and 100k DoF for 2D and 3D case respectively.
- MOR also allows to take advantage of exporting the model as an electric two-port device, due to the fact that the limit on the number of equations inside the model-container VHDL file is not a hurdle anymore, and hence the model can be easily imported in electric-circuit simulation tools, such as Simplorer.

Conclusions and Outlook

- Frequency splitting was analysed, and its approximated values were calculated in a scenario where all the resistances are equal to zero, showing to be in the close range to those provided by the resulting data in Simplorer. Finally, it was observed a maximum in the transfer of power was held for all the calculated frequency range.

- A slight difference in axis misalignment above a certain threshold, proved that affected the power efficiency more than a vertical displacement, mainly because both coils had the same diameter, and this issue was notoriously magnified in the range of 50 – 250 mm, where the values were affected by magnetic fields flux in a reverse direction

- For this issue, one possible solution would be to increase the diameter size of the primary coil, or perhaps to investigate other different geometries (e.g. solenoid type , bipolar solenoid, unipolar rectangular and bipolar rectangular).

THANK YOU FOR YOUR ATTENTION !